

Correspondence

Classifying elephant behaviour through seismic vibrations

Beth Mortimer^{1,2,*}, William Lake Rees³, Paula Koelemeijer³, and Tarje Nissen-Meyer³

Seismic waves — vibrations within and along the Earth’s surface — are ubiquitous sources of information. During propagation, physical factors can obscure information transfer via vibrations and influence propagation range [1]. Here, we explore how terrain type and background seismic noise influence the propagation of seismic vibrations generated by African elephants. In Kenya, we recorded the ground-based vibrations of different wild elephant behaviours, such as locomotion and infrasonic vocalisations [2], as well as natural and anthropogenic seismic noise. We employed techniques from seismology to transform the geophone recordings into source functions — the time-varying seismic signature generated at the source. We used computer modelling to constrain the propagation ranges of

elephant seismic vibrations for different terrains and noise levels. Behaviours that generate a high force on a sandy terrain with low noise propagate the furthest, over the kilometre scale. Our modelling also predicts that specific elephant behaviours can be distinguished and monitored over a range of propagation distances and noise levels. We conclude that seismic cues have considerable potential for both behavioural classification and remote monitoring of wildlife. In particular, classifying the seismic signatures of specific behaviours of large mammals remotely in real time, such as elephant running, could inform on poaching threats.

The propagation of seismic information is affected by the vibration source, which in this study is elephant behaviour. Seismic vibrations generated by wild elephants were recorded in Kenya (Supplemental information). We selected a few examples of each observed behaviour type, as well as car noise, which were processed to determine the corresponding source function — the force strength and pattern generated by the elephant ‘at the source’ (Supplemental information). Differences in elephant behaviour caused detectable changes in source function properties, which remained

distinguishable during modelled seismic wave propagation up to 1000 metres regardless of the noise level and terrain type (Figure 1; Supplemental information). Recordings of seismic vibrations can therefore be used to classify elephant behaviours.

Besides vibration generation behaviour, seismic information transfer is also affected by physical factors during propagation, such as background seismic noise and terrain type [1]. We employed modelling software used in modern seismology [3], which provides benefits over previous modelling approaches [2,4] as it computes realistic and accurate frequency-dependent wave propagation, using source functions and local geological information for the elephants’ home range as model inputs (sand or weathered gneiss (a type of solid rock) in the top 25 metre layer; Supplemental information).

Using the set of source functions and a seismological detectability technique, we determined the maximum propagation range where cues could be detected above recorded background noise levels. For our set of source functions, vocalisation behaviours gave higher input forces and hence larger propagation ranges compared to locomotion (Supplemental information).

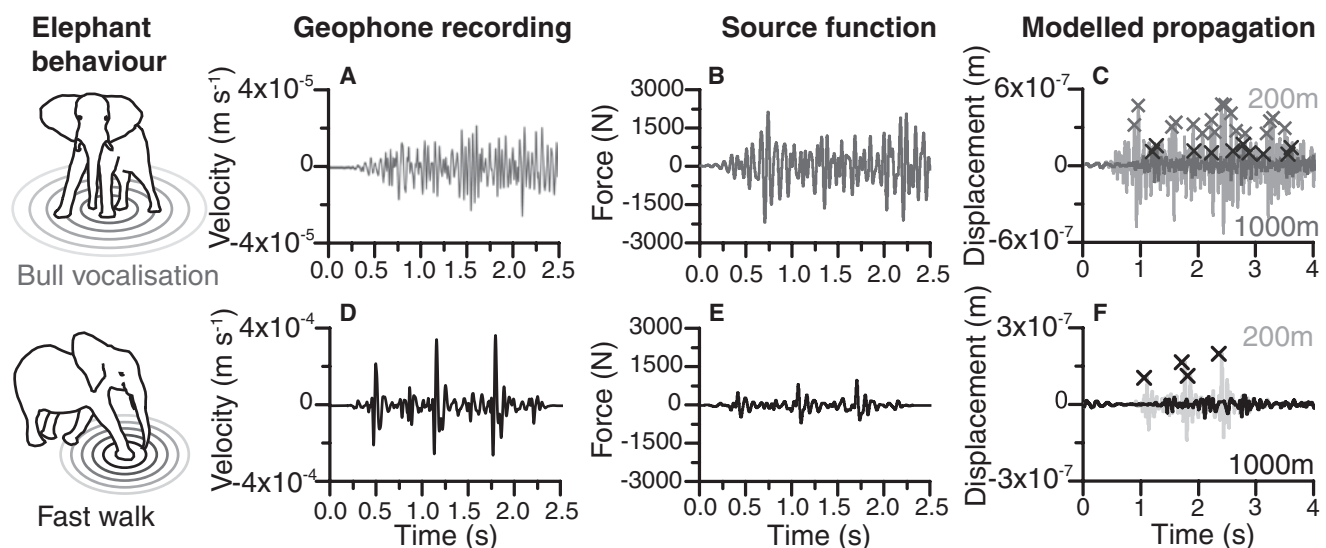


Figure 1. Determining the propagation of seismic forces produced by elephant behaviours.

A rumble from a bull (A, B, C) versus each footfall in a fast walk (D, E, F) differs in recorded vertical ground velocity versus time (A, D), determined source function force versus time (B, E) and modelled propagation sampled at 200 m and 1000 m from the source (modelled with high noise on sandy terrain; C, F). Scatter points in C (lighter for 200 m and darker for 1000 m) and F indicate points that are higher than half the maximum peak amplitude. Only fast walk at 1000 m is not detectable over background noise (Supplemental information). Note different axes scales between A and D and C and F.

Maximum propagation range estimates were 6.4 km for cow rumble versus 3.6 km for fast elephant walk (maximum seismological force 2546 N versus 946 N respectively). Faster gaits of larger elephants will generate higher forces [5, 6], thus leading to a larger propagation range. A sand top layer increases the propagation range for each behaviour compared to a gneiss top layer, so is best suited for long-range information transfer (Supplemental information). However, superimposing ambient noise that was high relative to other noise recordings in the field (mixture of natural and anthropogenic sources) significantly decreased the detectable propagation range (84% \pm 16% lower under higher noise on average) and thus limits information transfer (Supplemental information).

Our findings have implications for the study of seismic information transfer between elephants. Firstly, our results suggest that elephants have the option of using the seismic component of rumbles for long-range communication (over 3 km) [2,7]. Long-range information transfer is also possible through high-force locomotion behaviours. Rapid running in elephants is a sign of distress or aggression [8], and we estimate that these high-force behaviours will propagate over many kilometres, potentially providing useful information to promote vigilance in spatially-separated elephant groups. In addition, we found an added benefit of river sand, as background noise is reduced (Supplemental information), and seismic cues propagate with less energy loss compared to other terrains in the elephants' home range. Whether this applies to kilometre-range scales in the field remains to be quantified.

The last step in the information transfer process, seismic vibration detection, requires more research in elephants and other animals. Elephants have been shown to discriminate between the seismic components of vocalisations [7], but more research is required on the ability to discriminate between sources (behaviour, identity and single/multiple) in different physical contexts (distance from source, noise level, substrate properties). Additionally, more organisms are likely to be sensitive to seismic vibrations than are currently reported. If so, seismic vibrations can be used as

biological information during ecosystem interactions. However, the strong limiting effect of noise raises concerns over the implications of close-range anthropogenic seismic sources on this mode of information transfer, for example car noise in the 20–25 Hz range (Supplemental information).

Finally, our results support the notion that seismic recording is an intriguing, non-intrusive option for remote monitoring of wildlife, particularly large mammals [9]. Real-time monitoring of poacher threat in remote landscapes is important for species conservation [10], and we suggest that detection of rapid runs could be used in this context. In particular, utilising multiple geophones with algorithms for detection and discrimination of seismic cues could be implemented for real-time monitoring (Supplemental information). This technique can distinguish spatially-separated seismic sources by determining their locations. The chosen geophone number and spatial separation will depend on the range and spatial resolution required, where higher geophone sensitivity, lower ambient noise level and variance, and higher force magnitude of the behaviour will lead to a greater detection range and discrimination accuracy. More data are required to develop and robustly test these methods in practice, which has potential applications within a range of wildlife monitoring contexts.

SUPPLEMENTAL INFORMATION

Supplemental Information including experimental procedures, one figure and one table can be found with this article online at <https://doi.org/10.1016/j.cub.2018.03.062>.

ACKNOWLEDGEMENTS

All authors thank Iain Douglas-Hamilton, George Wittemeyer and all the staff at Save the Elephants for kindly agreeing to support the fieldwork in Kenya. BM thanks Fritz Vollrath for suggesting the study and his valuable discussions throughout; she also thanks the John Fell Fund, Oxford's Jesus College, and the Royal Commission for the Exhibition of 1851 for funding. WLR thanks the Department of Earth Sciences and Oxford's St Anne's College for funding. All authors acknowledge funding from and discussions within the European Union's Horizon 2020 Research and Innovation Programme WAVES under the Marie Skłodowska-Curie Grant

641943. PK thanks Oxford's University College for funding. We thank Dr Kuangdai Leng, the main author of the seismic computer software AxiSEM3D (github.com/axisem3D, axisem.info), for his help throughout the M.Sc. project of WLR, as well as further Oxford seismology group members Dr Kasra Hosseini, Maria Tsekhmistrenko and Alexandre Szenicer for their support in the seismic processing.

AUTHOR CONTRIBUTIONS

B.M. and T.N.M. initiated the project and T.N.M., P.K. and B.M. designed field experiments. B.M. and W.L.R. collected field data. T.N.M., P.K. and W.L.R. analysed seismic recordings and implemented computer models. B.M. wrote the manuscript and all authors edited the manuscript.

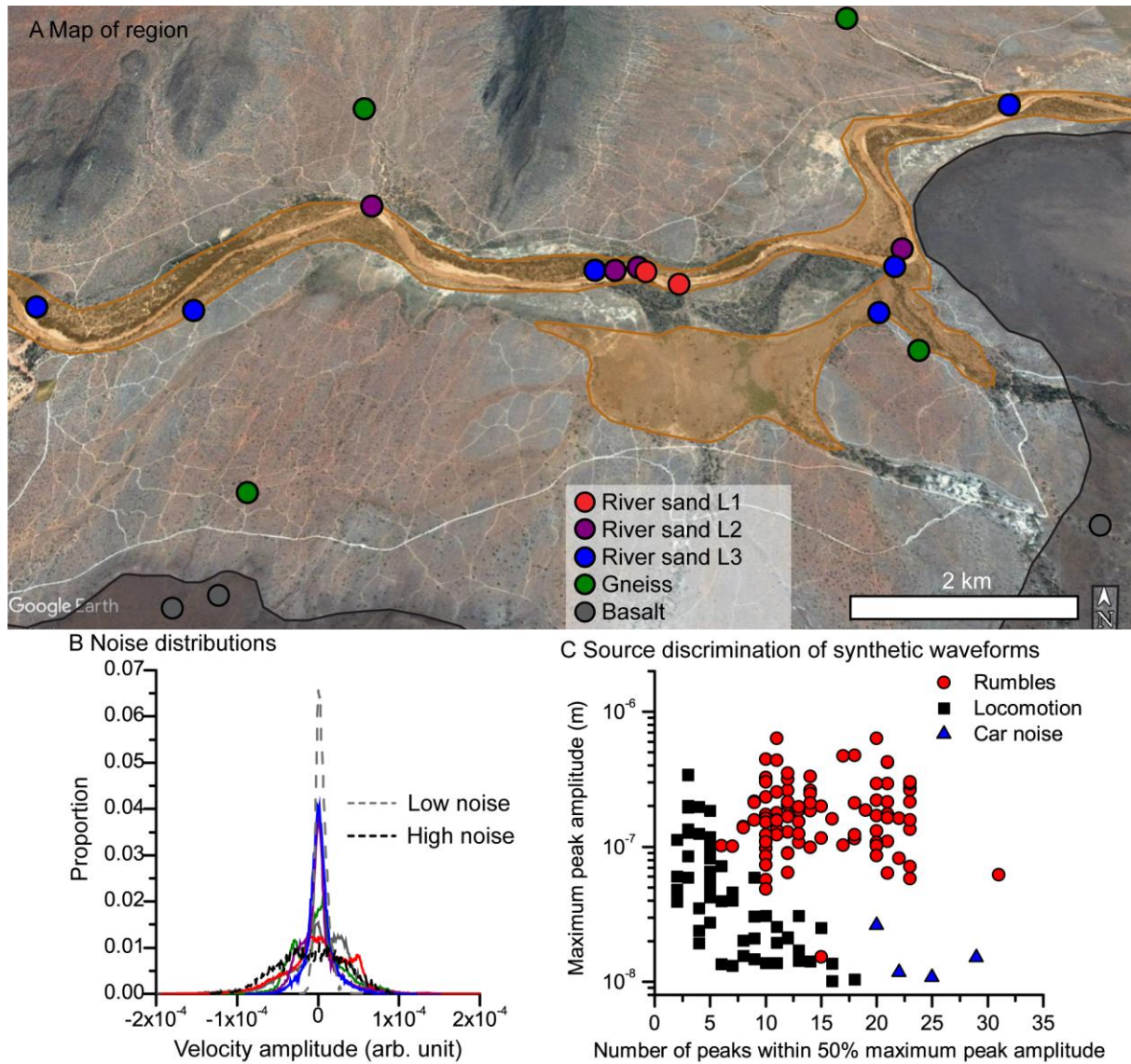
REFERENCES

- Mortimer, B. (2017). Biotremology: Do physical constraints limit the propagation of vibrational information? *Anim. Behav.* **130**, 165–174.
- O'Connell-Rodwell, C.E., Arnason, B.T., and Hart, L.A. (2000). Seismic properties of Asian elephant (*Elephas maximus*) vocalizations and locomotion. *J. Acoust. Soc. Am.* **108**, 3066–3072.
- Leng, K., Nissen-Meyer, T., and van Driel, M. (2016). Efficient global wave propagation adapted to 3-D structural complexity: A pseudo-spectral/spectral-element approach. *Geophys. J. Int.* **207**, 1700–1721.
- Günther, R.H., O'Connell-Rodwell, C.E., and Klemperer, S.L. (2004). Seismic waves from elephant vocalizations: A possible communication mode? *Geophys. Res. Lett.* **31**, L11602.
- Ren, L., Miller, C.E., Lair, R., and Hutchinson, J.R. (2010). Integration of biomechanical compliance, leverage, and power in elephant limbs. *Proc. Natl. Acad. Sci. USA* **107**, 7078–7082.
- Ren, L., and Hutchinson, J.R. (2008). The three-dimensional locomotor dynamics of African (*Loxodonta africana*) and Asian (*Elephas maximus*) elephants reveal a smooth gait transition at moderate speed. *J. R. Soc. Interface* **5**, 195–211.
- O'Connell-Rodwell, C.E., Wood, J.D., Kinzley, C., Rodwell, T.C., Poole, J.H. and Puria, S. (2007). Wild African elephants (*Loxodonta africana*) discriminate between familiar and unfamiliar conspecific seismic alarm calls. *J. Acoust. Soc. Am.* **122**, 823–830.
- Sukumar, R. (2003). *The living elephants: Evolutionary ecology, behavior, and conservation* (New York: Oxford University Press).
- Wood, J.D., O'Connell-Rodwell, C.E., and Klemperer, S.L. (2005). Using seismic sensors to detect elephants and other large mammals: A potential census technique. *J. Appl. Ecol.* **42**, 587–594.
- O'Donoghue, P., and Rutz, C. (2016). Real-time anti-poaching tags could help prevent imminent species extinctions. *J. Appl. Ecol.* **53**, 5–10.

¹School of Biological Sciences, University of Bristol, Bristol, BS8 1TQ, UK. ²Department of Zoology, University of Oxford, Oxford, OX1 3PS, UK. ³Department of Earth Sciences, University of Oxford, Oxford, OX1 3AN, UK. *E-mail: beth.mortimer@zoo.ox.ac.uk

Supplemental Information: Classifying elephant behaviour through seismic vibrations

Beth Mortimer, William Lake Rees, Paula Koelemeijer, Tarje Nissen-Meyer



Supplemental Figure S1. (A) Map of recording locations in Samburu and Buffalo Springs National Reserves in Kenya. Colour gives the geology type: red, purple and blue are river sand level (L) 1, 2, and 3 respectively (shaded orange on map), green is gneiss (not shaded on map) and grey is basalt (shaded grey on map). White bar denotes 2 km. (B) The distributions of all noise recorded on the five substrate types in the field (solid lines), with the distribution of two recordings plotted with dashed lines, which were chosen as representative of low noise (grey) and high noise (black) for the computer modelling. (C) Plot showing method to discriminate synthetic waveforms based on number of peaks within 50% of the maximum peak amplitude for each waveform (x axis) and the maximum peak amplitude of each waveform (y axis) for six rumbles (red circles), six walks/steps (black squares) and car noise (blue triangles). Inputs into the computer models were source functions and substrate of sand or gneiss, and the model outputs were synthetic waveforms sampled at 200, 400, 600, 800 and 1000 m from the source overlaid with high or low noise (see also Supplemental Table S1). Only synthetic waveforms that were detectable over background noise through STA/LTA analysis were used.

Supplemental Table S1. Source function properties and modelled maximum propagation ranges of different elephant behaviours. Seismic motions elicited by different elephant behaviours (and car noise for comparison), which differed in force and frequency content, were inputted into the modelling. Structural input models differed in the top 25 m layer, which was either gneiss or sand. Model outputs were overlaid with longer term measured high or low noise. Maximum propagation range was defined as the maximum distance at which a short term averaging to long term averaging ratio (STA/LTA) threshold of 1.6 was triggered when using a 200 m resolution.

Behaviour ^a	Source function properties		Top 25 m layer in model	Frequency band	Range (m)									
	Max. force (N)	Dominant Frequency Range (Hz)			All frequencies (4.5-25 Hz)		5-10 Hz		10-15 Hz		15-20 Hz		20-25 Hz	
					Noise Level	Low	High	Low	High	Low	High	Low	High	
Walk 1 (adult 1)	279	10-15	Gneiss		1000	0	600	0	2000	0	1400	0	1600	200
Walk 2 (young 1)	273	10-15	Gneiss		400	0	200	0	1400	0	1000	0	1600	400
Walk 3 (adult 2)	125	20-25	Gneiss		400	0	0	0	1200	0	600	0	1000	0
Walk 4 (adult 3)	946	5-10	Gneiss		1800	200	1400	0	2800	400	2400	200	2800	1200
Walk 5 (young 2)	289	10-15	Gneiss		800	0	200	0	1800	0	1200	0	1400	200
Climbing step	1190	20-25	Gneiss		1800	200	400	0	1800	0	2800	600	3200	1400
Bull 1 rumble 1	1314	20-25	Gneiss		4400	1200	3400	200	5600	2000	3800	1400	3000	1200
Bull 1 rumble 2	2546	10-15	Gneiss		4200	1400	3000	200	6000	2400	5200	2200	4200	2200
Bull 1 rumble 3	2100	5-10	Gneiss		4400	1200	3200	200	5400	2400	4800	2200	4200	2200
Cow 1 rumble 1	69	10-15	Gneiss		0	0	0	0	200	0	200	0	600	0
Cow 2 rumble 2	2238	10-15	Gneiss		4400	1400	3200	400	6000	2600	4800	2200	4600	2800
Cow 2 rumble 3	1401	5-10	Gneiss		3600	800	2600	200	4200	1800	4400	1200	3000	1600
Car	88	20-25	Gneiss		200	0	0	0	0	0	800	0	1400	200
Walk 1 (adult 1)	279	10-15	Sand		1600	0	1000	0	2400	200	2000	400	2000	800
Walk 2 (young 1)	273	10-15	Sand		1000	0	200	0	1800	200	1800	200	2200	1000
Walk 3 (adult 2)	125	20-25	Sand		800	0	200	0	1600	0	1200	0	1400	200
Walk 4 (adult 3)	946	5-10	Sand		2400	400	1800	0	3600	1200	3000	600	3200	1800
Walk 5 (young 2)	289	10-15	Sand		1400	0	600	0	2200	200	1800	200	2200	800
Climbing step	1190	20-25	Sand		2200	600	800	0	2400	200	3400	1400	3400	1800
Bull 1 rumble 1	1314	20-25	Sand		4600	1600	3800	600	6000	2800	4200	2000	3200	1600
Bull 1 rumble 2	2546	10-15	Sand		4600	2000	3600	800	6200	3000	5400	2800	4200	2600
Bull 1 rumble 3	2100	5-10	Sand		4800	1800	3400	600	6000	3000	5000	2600	4200	2800
Cow 1 rumble 1	69	10-15	Sand		200	0	0	0	400	0	800	0	1000	0
Cow 2 rumble 2	2238	10-15	Sand		5200	2000	3800	600	6400	3400	5600	2600	4800	3200
Cow 2 rumble 3	1401	5-10	Sand		4000	1400	3000	600	5400	2800	4800	2200	3800	2000
Car	88	20-25	Sand		600	0	0	0	200	0	1400	0	2000	800

^aWalks were chosen as they included the maximum, minimum and median maximum forces during that recording.

Supplemental Experimental Procedures

1. Geophone recordings of seismic noise and elephant behaviour

One geophone (RTC-4.5Hz-395 vertical, USA) sensitive to vertical ground motions was used to record seismic vibrations. We recorded background seismic noise at 19 different locations (Supplemental Figure S1A) and elephant behaviours at 32 locations in the field in Samburu and Buffalo Springs National Reserves in northern Kenya. The geophone was connected to a DAQ unit (VIB-E-220, Polytec, GmbH), which plugged into a laptop running VibSoft (v.5.0, Polytec, GmbH). Sampling frequency was 600 Hz, giving a time resolution of 1.67 ms. Voltage-time profiles were then converted to velocity by multiplying by a calibration factor (set by hardware) of $23.4 \text{ V m}^{-1} \text{ s}^{-1}$.

GPS location, temperature, humidity, geology and soil type were recorded for each location. During elephant recordings, we also obtained video and audio data using a hand-held camera (Olympus TG-3), which were synchronised with the geophone recordings. We used a digital range finder (GRANDBEING CP-80S) to record distance from the geophone to the elephant during the observational period, and measured distances with a tape measure retrospectively, where required. We subsequently analysed the data to categorise the behaviour of the elephant closest to the geophone, time and geophone peak amplitude. The effects of propagation distance and local damping on the velocity amplitude were accounted for when determining the source functions.

We recorded a range of elephant individuals, from lone males to mixed-age family groups across a two-week period within the two National Reserves, making recordings from an average of 14 different individuals on each day (number of elephants per day ranged from 5 to 31; the same individuals are likely to have been recorded on separate days). To avoid interference between multiple elephants, we positioned the geophone close (range of 2 to 30 m) to a focal individual or in a position where we could record an individual as it passed by. Such interference can be dealt with using spatially separated geophones that allow coherence analysis to discriminate between single and multiple sources, which works best if source separation is maximised and temporal overlap is minimised. However, this was not practical for our field work, as we frequently moved location due to time constraints. Recording was typically in the late afternoon (3pm-6pm), when the elephants were exhibiting more active behaviours such as grazing, vocalising and walking. During this time, elephants were mostly on river sands, but we also obtained recordings from elephants on gneiss (a hard rock type). As this study involved only observations of behaviour and recordings of ground-based vibrations, with no disruption of the habitat, no specific ethical approval was required. Permission to carry out the fieldwork was obtained from the National Commission for Science, Technology & Innovation, Kenya (permit number NACOSTI/P/16/69501/9147). We also recorded the noise generated by a car as it moved towards and away from a geophone (moving at c. 10 mph), which was 4 m away at its closest point.

Three geology types were identified across the field locations, including gneiss and basalt (both rocks) and river sand (Supplemental Figure S1A). River sands were classified into three different levels, where level 1 had the lowest elevation relative to the river bed, and level 3 had the highest elevation. A higher elevation from the river bed was accompanied by a more consolidated sand layer, less loose sand covering, and more vegetation.

Noise is generated by natural (biotic and abiotic, e.g. other animals or geological processes) and anthropogenic (e.g. car noise, human activity) sources and our recordings in the field measured the seismic noise caused by a mixture of sources from a variety of locations. The detection of noise will be dictated by the sensitivity of the seismic sensor, as well as its coupling with the substrate. More sources of noise, higher amplitude sources or being close to a specific seismic source will interfere with seismic information transfer as the signal-to-noise ratio drops. Recordings of noise were grouped by the five terrain types (basalt, gneiss, river sand levels 1, 2 and 3). A distribution was then calculated using a grouping of velocity amplitude of the noise of 1×10^{-6} (arbitrary unit), where the number of data points within each amplitude grouping was expressed as a proportion of all the data points (N= 76980, 83112, 80196, 51726 and 40500 for basalt, gneiss, river sand levels 1, 2 and 3 respectively). The distributions are shown in Supplemental Figure S1B along with distributions of two recordings that were chosen to represent 'high' and 'low' noise levels (recorded on river sand level 1 and 3 respectively). These recordings were chosen based on the range and variance of amplitudes present, picking the 2nd highest range and the 2nd lowest range out of all of the recordings with a low amplitude variance (thus avoiding extreme cases of high or low noise). These ambient background noise recordings are distinct from the recording of car noise (detailed above), as no specific vibration sources were close to the geophone.

2. Source function calculation

Seismic vibrations recorded at a distance from a source encode information from: (i) the time- and frequency-dependent source forcing and (ii) the properties of the traversed geological structures. Various methods exist to decouple these two influences and here we adopted the deconvolution method. This procedure requires the direct response of the structures due to a standard point source, in addition to the vibration recording for the unknown source and structures. The source function is then obtained by dividing the vibration recording by the direct response in the frequency domain. Deconvolution is an intricate and delicate data processing procedure, and future studies shall explore alternative robust approaches such as full source function inversion. However, for this a large data set is required.

In Kenya, the direct response was obtained by weight dropping experiments on-site. We measured the ground motion of the direct response caused by the weight dropping using two vertical geophones placed 2 and 6 m from the source. We calibrated the force generated through the weight dropping by using high-speed camera footage and force-motion equations. We utilised the deconvolution procedure across the recorded frequency range, on multiple sites, and for various types of forcing. With this method, we determined time- and frequency-dependent source forcing functions for elephant behaviours recorded at different locations and distances. We generated 13 source functions, including six rumbles (cow and bull), six types of steps (adult and juvenile), and recorded car noise. This gave a range of source function properties for each behaviour type (Supplemental Table S1), including a range of amplitudes. Note that for the walking behaviours each individual is different, but for the rumbles source functions are given from recordings for one bull and two cows. The inclusion of the car noise allowed a comparison of the seismic properties between elephant- and human-generated vibrations, which is important for the detection and discrimination of biological versus anthropogenic seismic sources.

3. Modelling

We used a novel seismic wave propagation method [S1] to compute seismic waveforms for geological structures that include property variations with depth and damping of seismic vibrations [S2]. For any given geological structure, this method delivers accurately modelled waveforms. We implemented multiple plausible geological models for the local region of Kenya, based on geological maps and on-site inspection. The chosen models varied only in depth, as well as the thin surface layer (either unconsolidated sand or gneiss) as those variations resulted in the largest first-order waveform effects. Computed seismic waveforms for each of the source functions were altered by overlaying field recordings of seismic noise, representing a ‘high’ and ‘low’ level (see section 1). Adding seismic noise to the computed waveforms for each recording distance simulated the arrival of the seismic signal in a natural setting.

The quantitative discrimination method of short term averaging/long term averaging (STA/LTA) was used to determine the maximum propagation range of each source function overlaid with high or low noise [S3]. The method discriminates between background (long term window) and possible signal (short term window) by monitoring the ratio between the averages in both windows. The range of the modelled seismic signal is determined as the maximum distance where the synthetic signal plus noise has an STA/LTA function whose maximum exceeds the critical STA/LTA triggering value. We used a short time window of 5 s and a long time window of 10 s with a triggering threshold ratio of 1.6. The triggering ratio was chosen to ensure that (i) seismic noise alone would not trigger a detection (due to the random nature of seismic noise the average of a short time interval should be similar to that of a longer time interval), and (ii) it allowed detection of a signal that was picked up through FFT analysis of waveforms (determined by eye). Importantly, unlike other discrimination methods, this analysis is more similar to the known physiological processes of mammalian hearing, where temporal summation and amplitude play a role in signal detection [S4].

The models sampled waveform propagation at 200 m intervals from the source up to 10 km. We used these outputs to generate synthetic waveforms for each of the four model input combinations (overlaid high or low noise, sand or gneiss top layer) for each of the source functions sampled at 200, 400, 600, 800 and 1000 m from the source. These synthetic waveforms formed a data set to study how we can discriminate between waveforms under different biological and physical contexts. We analysed the waveforms where the STA/LTA analysis showed that the signal was above background noise (as indicated in Supplemental Table S1). For this specific data set, a combination of two parameters allowed the discrimination of vocalisation versus locomotion versus car noise: the maximum peak amplitude and the number of peaks within 50% of the maximum peak amplitude (Supplemental Figure S1C). This discrimination method allowed the seismic waveforms to be classified into the three groups regardless of other properties of the source function, substrate type in the model and noise level, with minimal ambiguity (3 or 4 points overlapping out of 163). A larger data set and refined discrimination techniques will improve the discrimination procedure, taking into account frequency, amplitude and temporal

pattern of the waveform to: (i) be robust over a range of biological and physical contexts and (ii) provide a statistical measure of certainty of classification (see Section 4).

The modelled propagation ranges (Supplemental Table S1) encapsulate the extreme values for discriminating the seismic signals from background noise and can thus act as a predictive means for the maximal propagation range. Given the major influence of the stratified geological models, frequency content and background noise level on amplitude modulation, it is assumed that local 3D effects (e.g. geological enclosures, surface and subsurface topography, vegetation) have a small effect on amplitudes compared to geological end members (sand, rock, attenuation) and other factors (noise) considered here. Furthermore, no 3D geological models of Samburu or nearby regions exist to be tested directly, even though the method itself would allow for full 3D geological structures. The effect of 3D structures, most likely secondary to the parameter changes considered already, will thus be examined in a future study.

Although previous studies have modelled the propagation range of elephant-generated seismic waves [S5, S6], ours is the first to determine source functions for elephants and to numerically model the physics of seismic signals induced by elephants, including the frequency-dependence of wave propagation, and the influence of geological substrates, as well as realistic background noise. The wave propagation simulations were conducted for broadband signals spanning a frequency band between 4.5 and 25 Hz (Supplemental Table S1).

4. Suggested field approach of method

The STA/LTA method can be used in real time in the field, by monitoring geophone voltage outputs using a data logger that supports the simple STA/LTA algorithm function. With a larger data set, time window lengths and triggering threshold values could be optimised to biological (types and ranges of animals, or specific behaviours) and physical (geology and noise levels) contexts. Discrimination between triggered signals could then use algorithms taking into account the amplitude and frequency patterns over time, as used in previous seismic monitoring studies [S7, S8]. These algorithms need to be generated using large data sets as ‘training data’ that encompass a range of biological contexts (including co-generation of signals) and physical contexts (including a variety of propagation distances). The algorithm output will provide a classification of the waveform, along with a statistical certainty value. The algorithms will need to be tested, with observational data, for robustness before blind implementation and can be modified to suit a particular monitoring context as required. The implementation of these suggested detection and discrimination algorithms are possible in real time, allowing triggering and classification without the need to store large amounts of data.

The proposed techniques are much improved through the use of multiple geophones. With geophones in multiple locations, triangulation can be used to estimate the location of a seismic source. Accuracy will depend on geophone number and synchronisation, geophone sensitivity and time resolution, the known geological details for providing wavespeed values, as well as optimal geophone distribution. Knowing the location of a seismic source will also provide important information for specifying the triggering and classification algorithms (i.e. correcting for propagation distance when setting the detection threshold or discrimination characteristics). Furthermore, multiple geophones allow the use of coherence analysis, to determine whether a source is from a single location (e.g. single animal), or from multiple locations (multiple animals). Multiple geophones also allow seismic array techniques to be implemented that can boost weak signals.

As a final guide, we predict that the method will work well in certain scenarios better than others. In the best-case scenario, multiple geophones with good temporal and amplitude resolution would be used in terrain with known geological characteristics, to discriminate seismic sources that are high in force and generated in separate locations, with relatively constant noise low in amplitude. In the worst-case scenario, we would only have a single geophone with poor temporal and amplitude resolution, to identify seismic sources that are low in force and generated concurrently at any location, with variable noise present at high amplitude.

Supplemental References:

- S1. Nissen-Meyer, T., van Driel, M., Stähler, S., Hosseini, K., Hempel, S., Auer, L., Colombi, A., and Fournier, A. (2014). AxiSEM: Broadband 3-D seismic wavefields in axisymmetric media. *Solid Earth* 5, 425-445.
- S2. van Driel, M., and Nissen-Meyer, T. (2014). Optimized visco-elastic wave propagation for weakly dissipative media. *Geophys. J. Int.* 199, 1078-1093.
- S3. Sharma, B.K., Kumar, A., Murthy, V.M. (2010). Evaluation of seismic events detection algorithms. *J. Geol. Soc. India* 75, 533-538.
- S4. Heil, P., and Neubauer, H. (2003). A unifying basis of auditory thresholds based on temporal summation. *Proc. Natl. Acad. Sci. U.S.A.* 100, 6151–6156.

- S5. O'Connell-Rodwell, C.E., Arnason, B.T., and Hart, L.A. (2000). Seismic properties of Asian elephant (*Elephas maximus*) vocalizations and locomotion. *J. Acoust. Soc. Am.* *108*, 3066-3072.
- S6. Günther, R.H., O'Connell-Rodwell, C.E., and Klemperer, S.L. (2004). Seismic waves from elephant vocalizations: A possible communication mode? *Geophys. Res. Lett.* *31*, L11602.
- S7. Wood, J.D., O'Connell-Rodwell, C.E., and Klemperer, S.L. (2005). Using seismic sensors to detect elephants and other large mammals: A potential census technique. *J. Appl. Ecol.* *42*, 587-594.
- S8. Sugumar, S.J., and Jayaparvathy, R. (2013). An early warning system for elephant intrusion along the forest border areas. *Curr. Sci.* *104*, 1515-1526.